#240

J. Electroanal. Chem., 112 (1980) 97—115

POLYMER FILMS ON ELECTRODES

PART II. FILM STRUCTURE AND MECHANISM OF ELECTRON TRANSFER WITH ELECTRODEPOSITED POLY(VINYLFERROCENE)

PAMELA J. PEERCE * and ALLEN J. BARD **

Department of Chemistry, The University of Texas at Austin, Austin, TX 78712 (U.S.A.)

(Received 29th October 1979; in revised form 28th February 1980)

ABSTRACT

The structure and properties of electrodeposited poly(vinylferrocene) (PVF) films on platinum electrodes (PVF/Pt) were examined by electron microscopy, X-ray photoelectron spectroscopy, various electrochemical techniques and measurements of the film resistance. The data were consistent with a mechanism in which the polymer films are permeable to dissolved reactants. A theoretical treatment of this situation for chronoamperometry is presented. The oxidation and reduction of a variety of dissolved reactants with redox potentials far removed from that of the PVF/PVF$^+$ system at PVF/Pt occurred by diffusion of the electroactive species through the polymer film and subsequent reaction at the platinum surface.

INTRODUCTION

The preparation and characterization of polymer-coated electrodes have been described in a number of recent reports [1—17]. Adherence has been effected by adsorption and/or the negligible solubility of the polymeric material in the solvent employed [1,2,4,7,12—16] and by chemical bonding [3,5,6, 8—11,17]. In some cases, polymerization occurred on or at the electrode surface [1,2,6,10,16] or was induced in the presence of the electrode material by means of a glow discharge [8,9], a radio-frequency plasma [11] or by heating [17].

Although the effect of polymeric coatings on the electrochemical reactivity of solution reactants has been investigated [2,3,5,6e,7,8,10,11b,14—17], hard evidence concerning the mechanism of electron transfer to solution species at electrodes coated with polymeric films has been presented in relatively few cases [2,6e,8,14,15,17]. This problem is of some general importance because the same considerations apply to some of the other types of modified or derived electrodes (e.g. those produced by covalently binding molecules to the electrode surface to produce multilayers or thick films). Four different modes of reaction (e.g. reduction) of an electroactive species in solution, A, at a film-

* Present address: Occidental Research Corp., P.O. Box 19601, Irvine, CA 92713, U.S.A.
** To whom correspondence should be addressed.

covered electrode can be considered (Fig. 1): (A) electron (or hole) conduction through the film material itself with reduction of A occurring at the film–solution interface; (B) diffusion of A through pores or channels in the film with reduction of A occurring at the exposed substrate surface; (C) diffusion of A through the film material itself characterized by a diffusion coefficient, D_m, which may not be the same as that in solution, D_s, with reduction of A occurring at the electrode–film interface; (D) reduction of A by reduced electroactive groups in the film (mediated electron transfer). Mediated electron transfer is only possible when the polymer itself is electroactive [e.g. PVF, poly(*p*-nitrostyrene), poly(tetrathiafulvalene)] and the redox potential of the polymer half-reaction is sufficient to cause the reduction (or oxidation) of the solution species. Evidence of such mediated electron transfer has been reported [2,6e, 14,15,17].

In preliminary studies in these laboratories on the structure of electrodeposited poly(vinylferrocene) (PVF) films and on the behavior of dissolved, electroactive species at PVF/Pt electrodes, it was suggested that pores or pinholes in the polymer overlayer exist through which dissolved reactants could diffuse to the metal surface [7]. This paper is concerned with an examination

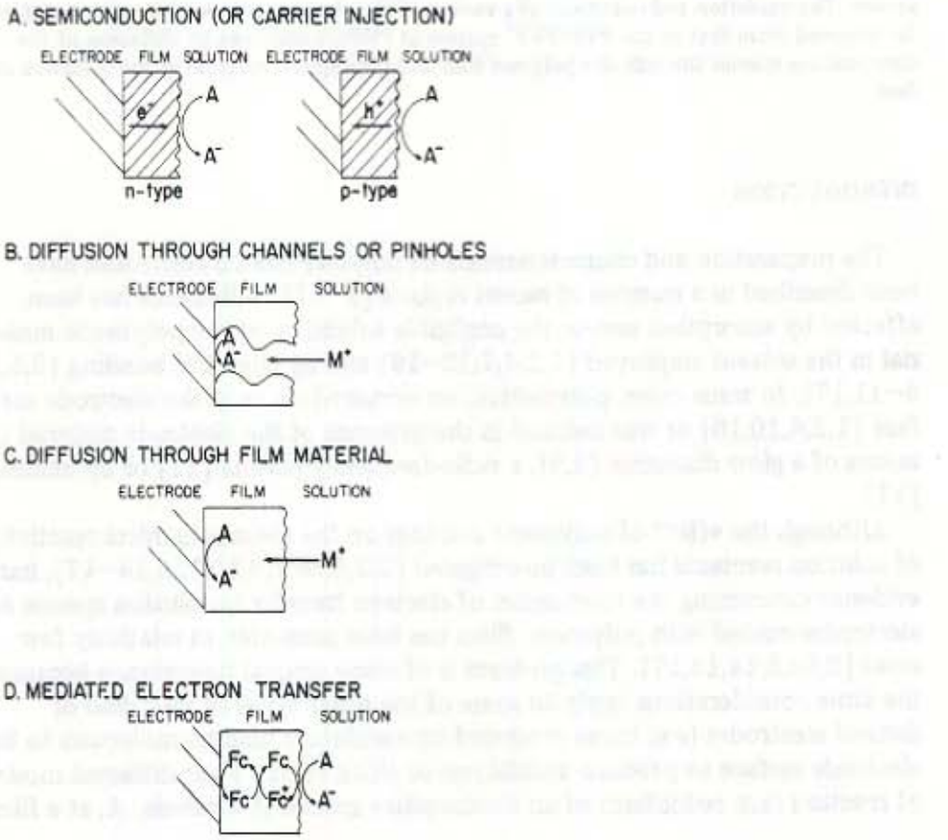

Fig. 1. Schematic presentation of possible reaction mechanisms of diffusing electroactive species at film-covered electrodes: A, electroactive species; M^+, counterion; e^-, electron; h^+, hole.

of the structure and properties of PVF films on platinum electrodes by electron microscopy, X-ray photoelectron spectroscopy, various electrochemical techniques and measurements of the film resistance with the purpose of obtaining mechanistic information about the redox reactions of solution species at polymer-coated electrodes. A related problem, the mechanism of oxidation and reduction of the polymer film itself, will be the subject of a separate paper from this laboratory.

EXPERIMENTAL

Materials

Acetonitrile (Matheson, Coleman and Bell) and methylene chloride (Fisher) were purified by several vacuum distillations over P_2O_5, which had been dried overnight on the vacuum line, and were stored in the glove box. Tetrabutylammonium perchlorate (TBAP) (Southwestern Analytical Chemicals) was recrystallized three times from 3 : 1 water : ethanol and dried for several days under vacuum. Here, 9, 10-diphenylanthracene (Aldrich) was sublimed once and zone refined twice.

Thianthrene (Aldrich) was recrystallized four times from benzene-methanol, once from acetonitrile and then sublimed. Chloranil (tetrachloro-*p*-benzoquinone) (Matheson, Coleman and Bell) was decolorized using carbon black and recrystallized three times from benzene. Poly(vinylferrocene) (PVF) (MW 15,700; degree of polymerization 74) was prepared and characterized by Dr. Thomas W. Smith [18].

All non-aqueous solutions were prepared in the glove box and contained 0.1 *M* TBAP as the supporting electrolyte. Aqueous solutions were degassed by bubbling with prepurified nitrogen.

Apparatus

All electrochemical measurements were made with a Princeton Applied Research (P.A.R.) Model 173 potentiostat, Model 175 universal programmer and Model 179 digital coulometer. Cyclic voltammograms were recorded on either a Houston Model 2000 X–Y recorder or a Tektronix Model 564 oscilloscope. Current–time transients were recorded on a Nicolet Model 1090A digital oscilloscope. The P.A.R. 173 and 179 were used to provide a constant current source for the four-point resistance measurements; the potential drop was measured using a Keithley Model 179 TRMS digital multimeter.

All experiments in non-aqueous solvents were performed in a Vacuum Atmospheres glove box under a helium atmosphere. A single-compartment cell was used. Unless otherwise specified, the working electrode was a platinum disk electrode (area 0.035 cm^2). A coiled piece of platinum wire or a piece of platinum foil served as the auxiliary electrode. Potentials in non-aqueous solvents are reported with respect to a silver wire quasi-reference electrode whose potential was 50 ± 10 mV negative of the aqueous SCE. Positive feedback techniques were employed in all experiments conducted in acetonitrile to compensate for solution resistance.

Electrochemical measurements in aqueous electrolytes were performed using a standard two-compartment cell which isolated the working and auxiliary electrodes. Potentials were measured and are reported with respect to the saturated calomel electrode (SCE).

All measurements were performed at the laboratory temperature, 25 ± 2°C. X-ray (Mg anode) photoelectron spectra were obtained with a Physical Electronics Model 548 Spectrometer (Eden Prairie, MN).

Procedure

Poly(vinylferrocene) was electrodeposited in its oxidized form as poly(vinylferrocenium) perchlorate onto a platinum disk electrode (for SEM, ESCA and conductivity measurements, platinum foil, 0.5 × 1.0 cm was used) from a stirred CH_2Cl_2 solution ca. 5 μM in PVF by maintaining the potential at 0.7 V without iR compensation. To achieve more uniform film deposition, the working electrode was surrounded by a cylindrical platinum foil counter electrode. The quantity of material deposited was controlled by the electrolysis times: 30—60 s, ca. 10^{-10} mol PVF cm^{-2}; 45—60 min, ca. 5×10^{-9} mol PVF cm^{-2}.

Platinum electrodes thus coated were removed from the polymer solution, shaken to remove any adhering solution and examined in acetonitrile solutions, in which both the neutral and oxidized films were insoluble, using cyclic voltammetry. The initial voltammograms were always identical to those obtained on subsequent scans, i.e. no break-in period was required for the PVF films in acetonitrile.

The average thickness, d, of the *dry* film was estimated from the charge, Q, consumed in completely reducing the film by stepping the potential from +0.9 to +0.2 V in acetonitrile solution, by the following equation:

$$d = QMW_{rp}/F\rho A$$

where MW_{rp} is the known molecular weight of the repeating unit, F the Faraday constant, A the geometric area of the electrode and ρ the density of the dry film. The density of the dry PVF film was taken to be the same as that of polystyrene, ~1 g cm^{-3}. If the PVF films swell in acetonitrile, their density would be $\leqslant 1$ and the polymer chains would penetrate much further into the solution than would be predicted from the estimated value of the dry film thickness. Consequently, the thickness values reported should be regarded only as indications of the minimum film thickness.

RESULTS

The electrodeposition of poly(vinylferrocene) (PVF) onto platinum electrodes was described in an earlier report from these laboratories [7]. Comparison of the cyclic voltammetry of 9, 10-diphenylanthracene (DPA) and 9, 10-anthraquinone at a platinum electrode prior to and following the deposition of 1.4×10^{-10} mol PVF cm^{-2} (dry film thickness, 30 nm) demonstrated that the polymer coating did not inhibit the redox processes of these diffusing reactants at scan rates of 0.2 V s^{-1} or less (Fig. 2). The results were the same for the experiment performed immediately following the deposition of a fresh coating

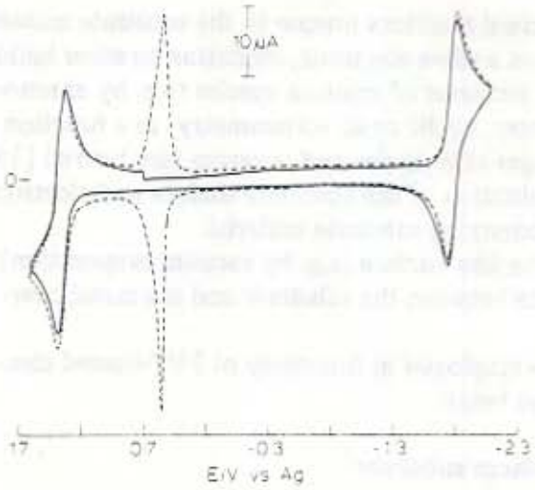

Fig. 2. Cyclic voltammogram of 1.06 m*M* 9,10-diphenylanthracene in acetonitrile/0.1 *M* TBAP at a platinum disk electrode, scan rate: 0.1 V s^{-1}. (———) On the blank platinum surface; (· · · · · ·) after electrodeposition of 1.4×10^{-10} mol cm^{-2} of PVF (dry thickness ~30 nm).

of PVF or after repeated cycling of the film in acetonitrile.

Further investigations on the effect of PVF films on the cyclic voltammetric behavior of dissolved reactants as a function of scan rate and film thickness were carried out with thianthrene as the dissolved reactant. At scan rates, v, <10 V s^{-1}, no increase in the peak potential separation, $\Delta E_p = E_{pa} - E_{pc}$, or decrease in the peak current functions, $i_p/v^{1/2}c$, for thianthrene was observed at Pt electrodes coated with ~10^{-10} mol PVF cm^{-2} (dry film thickness, 30 nm) (where E_{pa} and E_{pc} are the anodic and cathodic peak potentials, i_p is the peak current, and c is the concentration of dissolved reactant). At 50 V s^{-1}, the peak potential separation was 110 mV at PVF/Pt compared with 90 mV at bare platinum. Even when the polymer coating was at least several hundred nanometers thick (5×10^{-9} mol PVF cm^{-2}), the observed peak currents for thianthrene at 0.1 V s^{-1} at PVF/Pt were 95% of those obtained at the same electrode before polymer deposition and the peak potentials were separated by 60 mV.

The facile reduction of DPA at platinum electrodes coated with PVF cannot be attributed to efficient mediation of electron transfer by the polymer because the potential for the reduction of DPA to DPA^{-} is 2.3 V negative of that for PVF^{+} to PVF. Mediated electron transfer cannot satisfactorily explain the oxidation of thianthrene or DPA either, as the redox potentials for these reactions are ca. 0.75 V more positive than that for PVF oxidation. Consequently, it was previously proposed that DPA diffused to the electrode surface through pinholes or channels in the polymer film [7]. If these channels are of molecular dimensions, then these reactants were actually diffusing through the polymer film itself.

The demonstration of small holes or diffusion through the film is not as straightforward as first appearances might suggest, particularly if the holes are small and uniformly distributed. A number of general techniques can be envisioned to study the size and distribution of pinholes or channels in films on electrode surfaces:

(1) Observation of electrochemical reactions unique to the substrate material to demonstrate its exposure, e.g. on a silver electrode, oxidation to silver halide.

(2) Study of the voltammetric behavior of solution species (e.g. by chronoamperometry, chronopotentiometry, cyclic or ac voltammetry) as a function of time or frequency for certain ranges of hole size and coverage (are below) [19].

(3) Electron microscopic examination of the electrode surface and electron spectroscopic detection of the underlying substrate material.

(4) Deposition of a metal on the film surface (e.g. by vacuum evaporation) and measurement of the resistance between the substrate and the metal overlayer.

These various approaches were employed in this study of PVF-coated electrodes and the results are reported below.

Hydrogen adsorption on the platinum substrate

A property peculiar to platinum which was exploited to determine whether any of the underlying metal was still exposed after the deposition of PVF is the adsorption of hydrogen. Figure 3, curve 1, is a cyclic voltammogram in the hydrogen adsorption region for a platinum electrode which had been pretreated by repeated cycling between −0.28 and +1.25 V. The peaks arise from the reduction of protons to hydrogen adsorbed on different crystal faces of the polycrystalline electrode [20] and the steep rise in the current at potentials negative of −0.25 V signals the evolution of molecular hydrogen.

This pretreated electrode was then coated with 4.0×10^{-10} mol PVF cm^{-2}, the polymer film converted to its uncharged form by reduction at −0.1 V vs. Ag in 0.1 *M* TBAP/acetonitrile and the electrode reimmersed in 0.1 *M* H_2SO_4. After the polymer film had been broken in by repeatedly cycling between −0.10 and +0.80 V at $v = 1.0$ V s^{-1} until a steady-state voltammogram was ob-

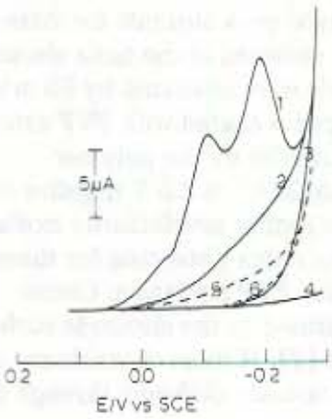

Fig. 3. Hydrogen adsorption region of cyclic voltammograms in 0.1 *M* H_2SO_4 at a platinum disk electrode, scan rate: 0.2 V s^{-1}. (———) (1) Bare platinum surface after cycling for 5 min between −0.28 and +1.25 V in same solution; (2) same electrode before cycling in 0.1 *M* H_2SO_4; (3) exponential fit to the steeply rising part of (1); (4) glassy carbon electrode of comparable area after electrodeposition of 5×10^{-10} mol PVF cm^{-2}. (· — · — ·) (5) Pretreated platinum electrode from (1) after electrodeposition of 4×10^{-10} mol of PVF; (6) exponential fit to the steeply rising part of (5).

tained and the area under the polymer waves equalled that observed in acetonitrile (ca 5 min), the potential was scanned to —0.30 V and curve 5 (Fig. 3) was recorded. When a bare Pt electrode was subjected to the same treatment in acetonitrile solution not containing PVF, the area under the curve in the hydrogen adsorption region was about the same as that observed before any cycling pretreatment (curve 2). Clearly the presence of the PVF film greatly attenuated the current attributable to hydrogen adsorption on Pt. Inspection of the PVF-coated electrode after the experiment of curve 5 by voltammetry in acetonitrile—0.1 *M* TBAP showed that the evolution of bulk hydrogen at ~—0.25 V caused the loss of approximately one-half of the PVF from the electrode surface.

The current observed in the region from 0 to —0.25 V in curve 5 arises from three sources: double-layer charging, hydrogen adsorption and hydrogen evolution. An estimate of the double-layer charging current is shown by curve 4 (Fig. 3) and was obtained from a voltammogram taken at a glassy carbon electrode coated with 5×10^{-10} mol PVF cm^{-2}, with the assumption that the double-layer capacities of glassy carbon and Pt are comparable. Because of the high hydrogen overvoltage of glassy carbon, the observed current can be attributed entirely to double-layer charging. The current—voltage curve for hydrogen evolution can be approximated by an exponential. An exponential fit of the steeply rising portion of curve 5 yielded curve 6.

In Fig. 3, curve 3 represents an estimate of the contribution of the hydrogen evolution current to curves 1 and 2. By integrating the areas bounded by curves 1, 3 and 4, 2, 3 and 4 and 5, 6 and 4, it was found that 386 $\mu C\ cm^{-2}$ of hydrogen was adsorbed on the pretreated platinum surface and ~150 $\mu C\ cm^{-2}$ on the acetonitrile-treated electrode compared with only 36 $\mu C\ cm^{-2}$ after deposition of PVF. Therefore, at most, 9—20% of the electrode was uncovered or the minimum fractional coverage by PVF, θ, was ~0.8. Since some PVF was lost from the surface during the experiment, this estimate of θ is considered to be a lower limit to the actual coverage. While this estimate is only very approximate, it proves useful in interpretation of the chronoamperometric results discussed below.

X-ray photoelectron spectroscopy (XPS) and electron microscopy

Oxidized PVF films ranging in thickness (dry) from approximately 20 nm to 0.5 μm were prepared as described in the experimental section, removed from the PVF—CH_2Cl_2 solution and analyzed by XPS to determine whether any of the underlying platinum substrate was exposed. The detection limit of the Pt 4f band was about 5 at.%. No platinum signals were observed for any of the PVF/Pt samples analyzed. Therefore, we conclude that in terms of exposed Pt the fractional coverage by PVF exceeded 0.95.

To show that the lack of detection of platinum bands for the PVF-coated samples could not be attributed to precipitation of TBAP on the electrode surface when the samples were removed from the polymer solution, additional samples were prepared and were dipped in acetonitrile to dissolve any precipitated TBAP prior to the XPS analysis. Once again, no platinum was detected. (A blank piece of platinum was also dipped in acetonitrile as a control; no

attenuation of the platinum bands was found.) In these latter experiments, since a larger number of sweeps was averaged to obtain the XPS spectrum, the detection limit improved to 2%. Therefore, θ exceeded 0.98 in the dry state.

Examination of a film of oxidized PVF approximately 0.3 μm thick (dry) by scanning electron microscopy (SEM) revealed the presence of numerous small channels in the polymer overlayer — the largest being approximately 0.5 μm in diameter (Fig. 4). Similar results were obtained when the beam was focused on several other areas of the polymer coating. Therefore, it is believed that the electron micrograph displayed in Fig. 4 is representative of the surface morphology of the dry PVF layer.

On repeated scanning of the electron beam over a given section of the sample, it was found that the size of the exposed areas gradually increased, indicating radiation damage of the polymer film. Since the photograph shown in Fig. 4 was taken on the second scan, radiation damage of this film was probably minimal.

Chronoamperometric measurements

Since the previously described measurements suggest very high surface coverage by the PVF, two alternatives, shown in B and C in Fig. 1 (diffusion through pinholes or through the film itself), are possible mechanisms for the observed electroactivity of solution species at the covered electrode. To investigate this

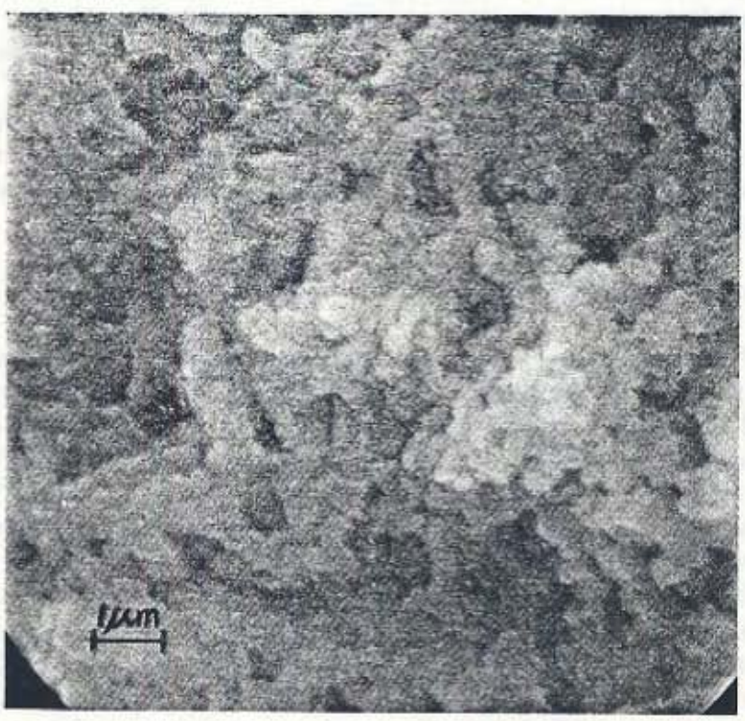

Fig. 4. Electron micrograph of poly(vinylferrocene) on platinum. Photograph taken during second scan. Approximate film thickness: 200–300 nm; magnification: 10,000x.

behavior and attempt to distinguish between these two models, potential-step chronoamperometric experiments were undertaken.

(1) The pin-hole model. Gueshi et al. [19a] have recently described the chronoamperometric behavior of diffusing reactants at an electrode surface partially covered by a thin insulating film. In their model, the electrode surface consists of uniformly distributed, circular, active regions of radius a separated by hexagonal, inactive regions (total unit radius R). The potential of the working electrode is abruptly stepped from some initial value at which the rate of reaction of the dissolved, redox species is negligibly slow to a potential at a which the reaction is diffusion controlled. As the electrolysis proceeds, the concentration of the diffusing reactant in the vicinity of the active regions is depleted and a diffusion layer forms around each active area.

The basic equation for the current for coverages, θ, >0.5, can be cast in a convenient dimensionless form from eqn. (31) in ref. 19a as:

$$\frac{i(\tau)}{i_d(\tau)} = \left(\frac{1}{\sigma^2-1}\right)\left\{\sigma \exp(-\tau) - 1 + \sigma^2\left(\frac{\pi\tau}{\sigma^2-1}\right)^{1/2} \exp\left(\frac{\tau}{\sigma^2-1}\right)\right.$$

$$\left. \times \left[\operatorname{erf}\left(\frac{\sigma\tau^{1/2}}{(\sigma^2-1)^{1/2}}\right) - \operatorname{erf}\frac{\tau^{1/2}}{(\sigma^2-1)^{1/2}}\right]\right\} \quad (1)$$

where $\sigma = \theta/(1-\theta)$, $\tau = lt$, $i_d(\tau)$ is the diffusion-limited current at the bare electrode and l is a function of the diffusion coefficient of electroactive species in solution, D, the hole size and distribution and θ, and is defined in ref. 19a. A plot of $i(\tau)/i_d(\tau)$ vs. log τ for $\sigma > 1$ ($\theta > 0.5$) (Fig. 5) shows that at short times when the thickness of the diffusion layer is small relative to the spacing between the exposed surface regions, the current ratio attains the limiting value of $(1-\theta)$. At long times, when the diffusion-layer thickness is large relative to the space between the active areas, the current ratio approaches unity. The actual time at which $i(t)$ deviates significantly (e.g by 5%) from $i_d(t)$ depends upon both θ and hole diameter. Representative plots of pinhole diameter required to yield a 5% deviation of the current from the bare electrode value for several values of θ, as a function of time, are shown in Fig. 6. These curves can be used to estimate the smallest detectable hole size for a given fractional coverage assuming that reliable measurements can be carried out down to times of 0.1–1 ms. For example, if θ = 0.95 (curve 4), holes 0.054 μm in diameter cannot be detected unless reliable data can be obtained for times less than ca. 0.4 ms. However, if θ were 0.98 (curve 5), these holes should be readily observable at times <5 ms. Smaller holes are more easily observed at higher fractional coverages, as is apparent from the curves in Fig. 5.

(2) Membrane model. The polymer film can also be treated as a membrane through which the solution electroactive species diffuses to the electrode surface. This can be treated as if the polymer layer were an immiscible liquid of thickness, δ, at the electrode surface (Fig. 7). The diffusion coefficient of the species in the polymer layer, D_m, differs from that in solution, D_s. Moreover, it is possible that a liquid–liquid extraction equilibrium occurs at the polymer–solution interface ($x = \delta$). If this is rapid at all times, the condition at the inter-

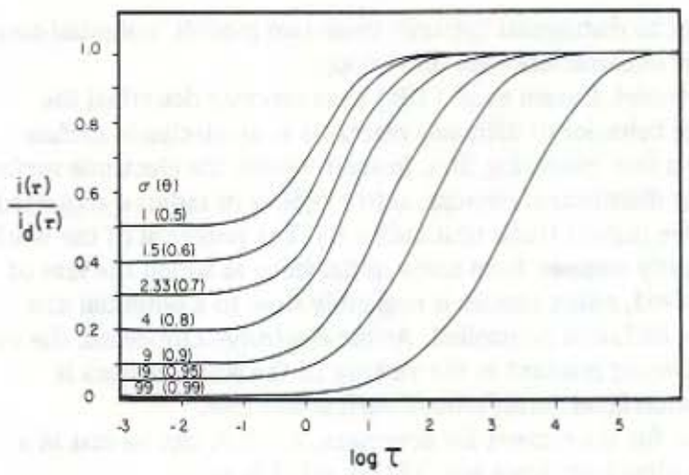

Fig. 5. Working curves based on pinhole model of Gueshi et. al. [19a] for $\theta \geq 0.5$ ($\sigma \geq 1$); $\tau = lt$.

face is

$$c_m(\delta, t) = c_s(\delta, t)K \tag{2}$$

where $c_m(x, t)$ and $c_s(x, t)$ are the concentrations of electroactive species in the polymer layer (m) and solution (s) respectively, and K is the extraction constant. Although problems relating to membranes on electrode surfaces and diffusion through them have been considered [21–23], to our knowledge a treatment of the chronoamperometric experiment in unstirred solutions has not yet appeared. The details of this model are given in the Appendix; the final equation in dimensionless form, is

$$\frac{i(\tau)}{i_d(\tau)} = a\left[1 + 2\sum_{j=1}^{\infty}\left(\frac{1-a}{1+a}\right)^j e^{-j^2/\tau}\right] \tag{3}$$

where $a = K(D_m/D_s)^{1/2}$ and $\tau = D_m t/\delta^2$. Calculated values of $i(\tau)/i_d(\tau)$ vs. $\log \tau$ for this model are given in Fig. 8. At short times the electrolysis is confined completely within the polymer layer and Cottrell behavior is followed with diffusion coefficient, D_m, and an initial concentration of Kc_s^*. Under these conditions the current ratio approaches $K(D_m/D_s)^{1/2}$. At longer times the diffusion layer is primarily in the solution phase, and $i(\tau)/i_d(\tau)$ approaches unity.

(3) Results. To examine the behavior of polymer-coated electrodes, the chronoamperometric oxidation of a 3.01 mM solution of thianthrene was performed at a platinum disk electrode before and after coating with 1.8×10^{-10} mol PVF cm^{-2}. The potential was stepped from +0.82 to +1.67 V and the current recorded as a function of time on a digital oscilloscope. The experiment was repeated twice and the data averaged. The use of short time data is limited by the rise time of the potentiostat–cell system and uncertainties in correcting the total measured current for the non-faradaic current attributable to double-layer charging. A correction for double-layer charging is generally carried out by repeating the potential step experiment under identical conditions in the supporting electrolyte solution alone, and subtracting the observed currents

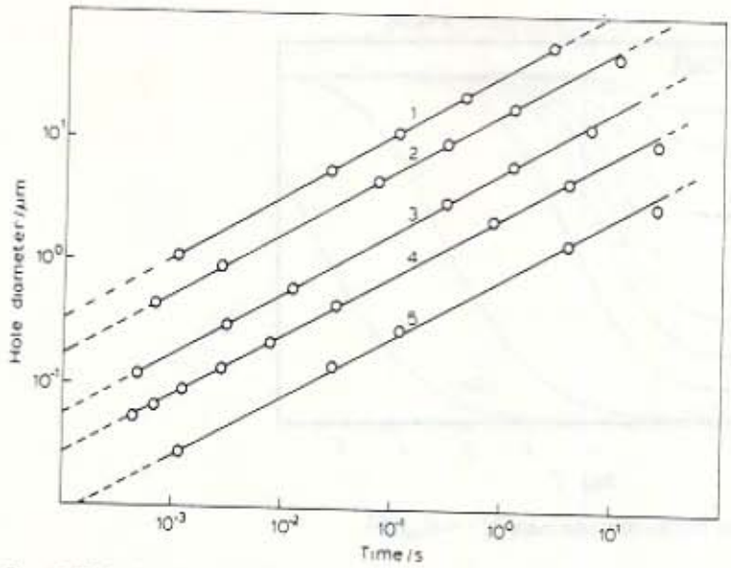

Fig. 6. Pinhole diameter plotted against the time at which the currents at the film-covered and blank electrodes are equal to within 5%. (1) $\theta = 0.70$; (2) $\theta = 0.80$; (3) $\theta = 0.91$; (4) $\theta = 0.95$; (5) $\theta = 0.98$.

from those measured in the presence of electroactive species. When this procedure was followed, the corrected data at a blank electrode exhibited Cottrell behavior, i.e. a plot of the faradaic current vs. $t^{-1/2}$ was linear, for times longer than ~1 ms. At shorter times, the observed faradaic current was greater than that expected from the Cottrell equation. The principal reason that this procedure fails to correct adequately for the charging current at times <1 ms is that it neglects the fact that even when the applied potential is constant, a change in the faradaic current will produce charging current [24]. As the faradaic current varies, the resulting potential drop across the uncompensated cell resistance, R_u, changes, causing the potential across the double layer to differ from the applied potential, thus inducing charging current. The total charging current, i_{c_t}, in the presence of a faradaic reaction is then the sum of the step charging current (that measured in the blank electrolyte), $i_{c_{step}}$, and the induced charg-

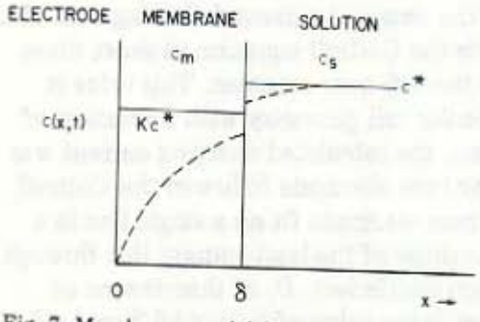

Fig. 7. Membrane model for polymer layer: (———) initial concentration profile; (- - - - - -) concentration profile after potential step.

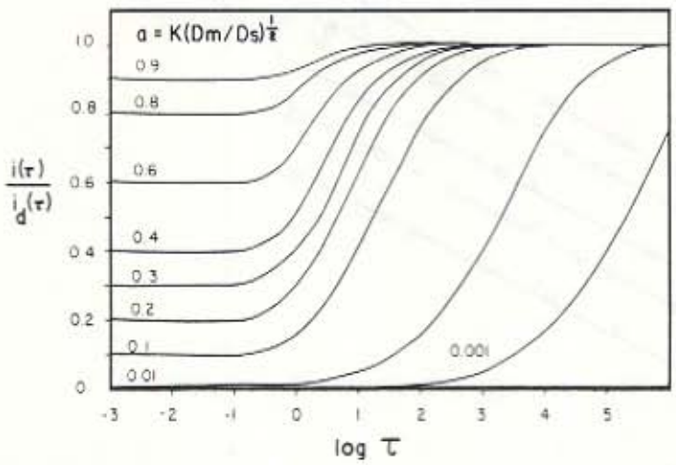

Fig. 8. Working curves for membrane model; $\tau = D_m t/\delta^2$.

ing current, $i_{c_{induced}}$:

$$i_{c_t} = i_{c_{step}} + i_{c_{induced}} \tag{4}$$

The total charging current may be calculated using the following equation given by Lai Miaw and Perone [25]:

$$i_{c_t}(t) = -R_u C_{dl} \frac{di_t(t)}{dt} \tag{5}$$

This allows the pure faradaic component of the total current to be obtained without a blank measurement.

Perone and coworkers [25,26] have experimentally demonstrated, in accordance with the theoretical model of Fratoni and Perone [24], that the faradaic current does not reach a maximum until about one time constant ($R_u C_{dl}$) after the potential step. Consequently, Cottrell behavior at a blank electrode cannot be observed until t is greater than several time constants. The acquisition of reliable data at short times is ultimately limited by the magnitude of the effective, uncompensated cell resistance. Use of high electrolyte concentrations (0.1—1 M) and placement of the reference electrode as near as possible to the working electrode will reduce the total R_u. The effective value of R_u can also be minimized by the use of positive feedback.

The averaged data were corrected for the charging current following eqn. (5). The best fit of the blank electrode data to the Cottrell equation at short times was obtained using a value of 200 μs for the cell time constant. This value is close to the time constant found for a similar cell geometry with a solution of only supporting electrolyte. At times 2 ms, the calculated charging current was negligible, and indeed the raw data on the bare electrode followed the Cottrell relationship. The corrected data for the bare electrode fit on a single line in a plot of i vs. $t^{-1/2}$ for times >0.4 ms. The slope of the least-squares line through these data yielded a value for the diffusion coefficient, D, of thianthrene of 1.89×10^{-5} cm^2 s^{-1}, in good agreement with the value of 2.01×10^{-5} cm^2 s^{-1} determined by cyclic voltammetry. In agreement with theory, the maximum faradaic current occurred at $R_u C_{dl}$, i.e. 200 μs.

The currents measured at the polymer-coated electrode were similarly corrected using the same value for the cell time constant. The assumption that the presence of the polymer film did not significantly change $R_u C_{dl}$ seemed justified by the observation that current–time curves recorded in the blank electrolyte before and after deposition of PVF were practically superimposable. Moreover, the maximum total resistance of the film, calculated by assuming a fractional coverage of >0.8 and solution channels (taking the specific conductivity of the 0.1 *M* TBAP/acetonitrile solution as 0.0134 Ω^{-1} cm^{-1} [27]) was negligible (1 Ω) compared to the overall cell resistance, even assuming significant swelling of the polymer layer. The double-layer capacitances of the coated and bare electrodes, as determined from cyclic voltammetry, were also essentially the same.

A plot of $i(t)/i_d(t)$ for the coated electrode vs. t is shown in Fig. 9. Clearly, at times ~1 ms the currents for the PVF-coated electrode are smaller than the uncoated one. While there is clearly some uncertainty in the data at short times, the fact that the coverage of the electrode is >0.8 suggests that the behavior corresponds more closely to the membrane model (Fig. 8) than the pinhole model (Fig. 5). Since measurements showing $i(t)/i_d(t) < 1$ should be possible at longer times if the film thickness is increased, this model can be better tested by studying the effect of film thickness on the observed behavior. Such experiments are currently under way in this laboratory and will be reported elsewhere.

Resistance measurements

To study the possibility of electronic conduction through the polymer layer, four-point resistance measurements [28] were conducted on dry PVF films (at least 0.2–0.3 μm thick) which had been electrodeposited onto platinum foil.

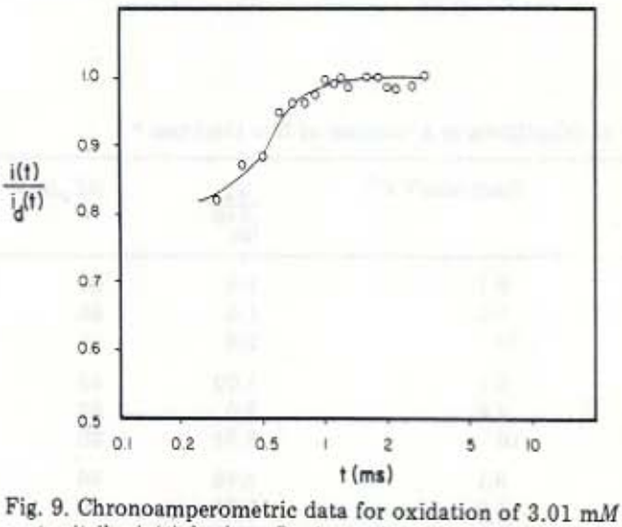

Fig. 9. Chronoamperometric data for oxidation of 3.01 m*M* thianthrene in 0.1 *M* TBAP–acetonitrile; $i_d(t)$ for bare Pt electrode; $i(t)$ for Pt electrode coated with 1.8×10^{-10} mol PVF cm^{-2} (dry thickness, ~40 nm). Potential step from +0.82 to +1.67 V. Data corrected for double-layer charging with eqn. (5).

The PVF/Pt samples were examined under a stereomicroscope (magnification 30×). A uniformly coated area approximately 1 mm^2 was selected and the rest of the electrode was carefully covered with glass cover slips. The samples were then placed in the vacuum evaporator and a layer of silver, approximately 0.5 μm thick, was evaporated on top of the exposed polymer film. One end of a piece of copper wire was then attached to the silver contact using silver paint. Silver paint was used to make connection to the voltmeter leads to minimize contact resistance. Constant currents of 0.02—0.5 mA (current densities, 0.2—4 mA cm^{-2}) were passed through the sandwich cell and the potential drop between the silver overlayer and the platinum substrate was measured. The resistance of the sandwich cell was 1.46 Ω. Therefore, if no macroscopic shorts of the silver overlayer to the underlying platinum occur, the conductivity of the oxidized PVF film (averaged over the 1 mm^2 area) is ~10^{-4} Ω^{-1} cm^{-1}. This conductivity can probably be attributed to Ag deposited in the pores (see the SEM results on a similar dry film sample) or to the bulk conductivity of the PVF film. Previous measurements of PVF conductivity have not been made, but the conductivity of poly(ferrocenylketone) was reported to be 10^{-3} Ω^{-1} cm^{-1} [29]. Therefore, the resistance measurements did not definitively rule out electronic conductivity in the PVF films. However, if the PVF films in acetonitrile exhibited such bulk conductivity, one would predict that the cyclic voltammeric behavior of a dissolved reactant such as thianthrene would be independent of the film thickness as long as the film resistance did not increase significantly or was compensated. However, if the reactant had to diffuse to the electrode surface through the PVF film, then the peak currents would decrease and the peak potential separation would increase as the film thickness increased [19b].

Consequently, the cyclic voltammetry of a 3.16 m*M* solution of thianthrene was investigated at platinum electrodes on which thick PVF films [approximate dry thickness, 0.1 μm (7.2×10^{-10} mol PVF cm^{-2}) and 0.5 μm (3.2×10^{-9} mol PVF cm^{-2})] had been deposited. Assuming that the bulk conductivity of the

TABLE 1

Cyclic voltammetric behavior of thianthrene as a function of film thickness [a]

	Scan rate/V s^{-1}	$\frac{i_{pa}}{i_{pa}^{\theta=0}}$	ΔE_p/mV
Bare Pt	0.1	1.0	60
	1.0	1.0	60
	10	1.0	80
>0.1 μm PVF/Pt	0.1	1.02	60
(7.2×10^{-10} mol PVF cm^{-2})	1.0	1.0	60
	10	0.92	80
>0.5 μm PVF/Pt	0.1	0.96	60
(3.2×10^{-9} mol PVF cm^{-2})	1.0	0.84	70
	10	0.71	90

[a] The solution contained 3.26 m*M* thianthrene and 0.1 *M* TBAP in acetonitrile.

oxidized PVF films in acetonitrile was 10^{-4} Ω^{-1} cm^{-1}, the resistance of these films would have been only 2 and 10 Ω respectively. Moreover, *iR* compensation was employed. Consequently, if thianthrene were oxidized at the polymer—solution interface rather than at the platinum surface, no difference in its behavior at the two polymer-coated electrodes would be observed. The results are shown in Table 1.

The ratio of the anodic peak currents at the film-covered and blank electrodes, $i_{pa}/i_{pa}^{\psi=0}$, decreased more sharply as a function of scan rate for the thicker film. For example, at 1 V s^{-1} this ratio was still unity for the 0.1 μm film, but only 0.84 for the 0.5 μm film. These results suggest that the oxidation of thianthrene does not occur at the film—electrolyte interface via electronic conduction in the film.

DISCUSSION

To explain the facile oxidation and reduction at PVF/Pt of various dissolved species whose redox potentials are far removed from that of PVF, a very general conduction mechanism is required. Efficient, fast mediated electron transfer (Fig. 10) required that the difference between the potentials of the mediator and reactant be not greater than ca. 180 mV [30]. Therefore, PVF may function as a mediator in some cases (ferrocenes are frequently used as mediators in electrochemical studies of biological redox molecules, e.g. see refs. 30 and 31), but electron transfer mediation is clearly not important in the redox reactions of thianthrene, DPA or 9, 10-anthraquinone at PVF/Pt.

The strong dependence of the cyclic voltammetric behavior of thianthrene on the thickness of films shows that electronic conduction (Fig. 1a) does not play a dominant role in the oxidation of thianthrene at platinum electrodes on which PVF has been electrodeposited. Diminution of the peak currents and increasing separation of the peak potentials with increasing film thickness is consistent with the operation of mechanisms B or C (Fig. 1). The distinction between electronic conduction and diffusion of the reactant through pinholes in the film has also been discussed by Tachikawa and Faulkner for gold electrodes on which metalized and metal-free phthalocyanines had been evaporated [32]. Some porosity of the electrodeposited PVF is supported by the hydrogen adsorption and SEM results, although the loss of film during these experiments makes these results a little ambiguous. The hydrogen adsorption peaks are peculiar to platinum, so that the observation of adsorbed hydrogen on platinum coated with PVF shows that part of the underlying metal is exposed to the solution. Observation of characteristic background reactions at polymer-coated electrodes has been reported by others. Oyama and Anson found that the reduction of quinone functionalities on the surface of pyrolytic graphite electrodes was not suppressed when these electrodes were coated with poly(vinylpyridine) [13b]. The complete inhibition of characteristic surface reactions of iron, copper and nickel electrodes coated with poly(tetracyanoethylene) metal chelate films was recently reported by Hiratsuka et al. [17] as evidence that the metal surfaces were completely covered by these films.

The chronoamperometric results, however, most strongly support the diffusion of reactant directly through the polymer layer, which can be thought of as

a viscous liquid layer swelled with solvent and supporting electrolyte ions, on the surface of the electrode. If the data of Fig. 9 are assumed to fit the membrane model of Fig. 5, then $K(D_m/D_s)^{1/2} \sim 0.8$ and $D_m/\delta^2 \sim 10^3\ s^{-1}$. Further estimates of the parameters of interest, D_m and K, are not possible without knowledge of the value of δ for the film swelled with solvent (which must be considerably greater than that of the dry film). It is also possible that both mechanisms B and C are operating and that the distinction between diffusion through the polymer layer, viewed as a homogeneous medium, and through tortuous channels of larger-than-molecular diameters in the film, is not easily drawn.

CONCLUSIONS

Electroreduction or oxidation of solution species whose redox potentials are far removed from that of PVF^+/PVF at electrodes on which poly(vinylferrocene) films are electrodeposited occurs via diffusion of the reactant through these films to the underlying substrate material. The existence of pinholes or channels must be considered when describing the behavior of surface modified and coated electrodes. The movement of ions through the film also plays a role in the electrochemical oxidation and reduction of the polymer film itself.

ACKNOWLEDGEMENT

The assistance of Dr. Michael Schmerling in obtaining the electron micrographs is gratefully acknowledged. We appreciate helpful suggestions and comments by Drs. Larry R. Faulkner and Steve Feldberg and the assistance of Edward D. Bard in theoretical computations. The support of this research by the National Science Foundation is gratefully acknowledged.

APPENDIX

Potential step chronoamperometry at membrane-covered electrode in unstirred solution — derivation of eqn. (3)

A number of papers have dealt with electrochemical measurements at membrane-covered electrodes [21—23] but none have dealt with the situation of interest here. For example, Mancy et al. [21] treat the case where a still liquid layer exists between the membrane and electrode with diffusion of reactant occurring in both phases, but assume the bulk solution phase is stirred. Earlier Bowers and Wilson [23] considered the simple membrane electrode in stirred solution. Rangarajan and Doss [22] investigated a situation similar to that discussed here, but they were concerned with the faradaic admittance and did not derive chronoamperometric equations.

We assume the model of Fig. 7. Mass transfer in both membrane and solution phases occurs by diffusion:

$$\frac{\partial c_m(x, t)}{\partial t} = D_m \frac{\partial^2 c_m(x, t)}{\partial x^2} \quad \text{(membrane)} \tag{A1}$$

$$\frac{\partial c_s(x, t)}{\partial t} = D_s \frac{\partial^2 c_s(x, t)}{\partial x^2} \qquad \text{(solution)} \tag{A2}$$

The initial conditions are:

$$c_s(x, 0) = c^* \qquad x > \delta,\ t = 0 \tag{A3}$$

$$c_m(x, 0) = Kc^* \quad 0 < x < \delta,\ t = 0 \tag{A4}$$

The boundary conditions are:

$$\lim_{x \to \infty} c_s(x, t) = C^* \tag{A5}$$

$$D_m\left(\frac{\partial c_m(x, t)}{\partial x}\right)_{x=\delta} = D_s\left(\frac{\partial c_s(x, t)}{\partial x}\right)_{x=\delta} \tag{A6}$$

If rapid transfer of electroactive species occurs at the membrane–solution interface, then distribution equilibrium is always maintained, so that

$$c_m(\delta, t) = Kc_s(\delta, t) \tag{A7}$$

For a potential step to potentials where the reaction rate is limited by diffusion,

$$c_m(0, t) = 0 \tag{A8}$$

The current at all times is given by

$$\frac{i(t)}{nFA} = D_m\left(\frac{\partial c_m(x, t)}{\partial x}\right)_{x=0} \tag{A9}$$

The Laplace transformation of (A1) and (A2) and application of conditions (A3), (A4) and (A5) leads to the equations:

$$\bar{c}_m(x, s) = A \exp(\sqrt{s/D_m}x) + B \exp(-\sqrt{s/D_m}x) + \frac{KC^*}{s} \tag{A10}$$

$$\bar{c}_s(x, s) = G \exp(-\sqrt{s/D_s}x) + \frac{C^*}{s} \tag{A11}$$

where $\bar{c}_m(x,s)$ and $\bar{c}_s(x,s)$ are the transformed concentrations $c_m(x,t)$ and $c_s(x,t)$, and A, B and G are constants to be evaluated. The transform of (A9) and substitution of (A10) yields:

$$\frac{\bar{i}(s)}{nFA} = (A - B)\, D_m^{1/2} s^{1/2} \tag{A12}$$

The constants A and B are evaluated with the boundary conditions (A6), (A7) and (A8) to yield the final equation:

$$\frac{\bar{i}(s)}{nFAKC^* D_m^{1/2}} = \bar{f}(s) = \frac{1 + w \exp(-ks^{1/2})}{s^{1/2}[1 - w \exp(-ks^{1/2})]} \tag{A13}$$

$$w = \frac{\gamma - K}{\gamma + K} \tag{A14}$$

$$\gamma = (D_s/D_m)^{1/2} \tag{A15}$$

$$k = 2\delta/D_m^{1/2} \tag{A16}$$

The term $[1 - w \exp(-ks^{1/2})]^{-1}$ can be expanded as a power series:

$$\bar{f}(s) = \frac{[1 + w \exp(-ks^{1/2})]}{s^{1/2}} \sum_{j=0}^{\infty} w^j \, e^{-jks^{1/2}} \tag{A17}$$

$$\bar{f}(s) = \frac{1}{s^{1/2}} + \sum_{j=1}^{\infty} \frac{2w^j \, e^{-jks^{1/2}}}{s^{1/2}} \tag{A18}$$

The inverse Laplace transform [33] finally yields:

$$\frac{i(t)}{nFAKC^* D_m^{1/2}} = (\pi t)^{-1/2} \left\{ 1 + \sum_{j=1}^{\infty} 2\left(\frac{\gamma - K}{\gamma + K}\right)^j \exp\left[\frac{-j^2\delta^2}{D_m t}\right] \right\} \tag{A19}$$

Since

$$\frac{i_d(t)}{nFAD_s^{1/2}C^*} = (\pi t)^{-1/2} \tag{A20}$$

combination of (A19) and (A20) yields

$$\frac{i(t)}{i_d(t)} = \left(\frac{K}{\gamma}\right) \left\{ 1 + 2 \sum_{j=1}^{\infty} \left[\frac{1 + (K/\gamma)}{1 - (K/\gamma)}\right]^j \exp\left(\frac{-j^2\delta^2}{D_m t}\right) \right\} \tag{A21}$$

By defining $a = K/\gamma$ and $\tau = D_m t/\delta^2$, eqn. (3) is obtained. This equation shows the following limiting behavior:

$t \to \infty \qquad i(t)/i_d(t) \to 1$

$t \to 0 \qquad i(t)/i_d(t) \to K/\gamma$

REFERENCES

1 (a) F. Bruno, M.C. Pham and J.E. Dubois, Electrochim. Acta, 22 (1977) 451; (b) M.C. Pham, P.C. Lacaze and J.E. Dubois, J. Electroanal. Chem., 86 (1978) 147; (c) M.C. *Idem*, Pham, J.E. Dubois and P.C. Lacaze, J. Electroanal. Chem., 99 (1979) 331.
2 H.L. Landrum, R.T. Salmon and F.M. Hawkridge, J. Am. Chem. Soc., 99 (1977) 3154.
3 A. Diaz, J. Am. Chem. Soc., 99 (1977) 5838.
4 (a) L.L. Miller and M.R. Van De Mark, J. Am. Chem. Soc., 100 (1978) 639; (b) *Idem*, J. Electroanal. Chem., 88 (1978) 437; (c) M.R. Van De Mark and L.L. Miller, J. Am. Chem. Soc., 100 (1978) 3223.
5 K. Itaya and A.J. Bard, Anal. Chem., 50 (1978) 1487.
6 (a) M.S. Wrighton, R.G. Austin, A.B. Bocarsly, J.M. Bolts, O. Haas, K.D. Legg, L. Nadjo and M.C. Palazzotto, J. Am. Chem. Soc., 100 (1978) 1602; (b) *Idem*, J. Electroanal. Chem., 87 (1978) 429; (c) J.M. Bolts and M.S. Wrighton, J. Am. Chem. Soc., 100 (1978) 5257; (d) M.S. Wrighton, M.C. Palazzotto, A.B. Bocarsly, J.M. Bolts, A.B. Fischer and L. Nadjo, J. Am. Chem. Soc., 100 (1978) 7264; (e) J.M. Bolts, A.B. Bocarsly, M.C. Palazzotto, E.G. Walton, N.S. Lewis and M.S. Wrighton, J. Am. Chem. Soc., 101 (1979) 1378.
7 A. Merz and A.J. Bard, J. Am. Chem. Soc., 100 (1978) 3222.
8 K. Doblhofer, D. Nolte and J. Ulstrup, Ber. Busensges. Phys. Chem., 82 (1978) 403.
9 D. Brosset, B. Ai and Y. Segui, Appl. Phys. Lett., 33 (1978) 87.
10 A.L. Allred, C. Bradley and T.H. Newman, J. Am. Chem. Soc., 100 (1978) 5081.
11 (a) R. Nowak, F.A. Schultz, M. Umaña, H. Abruña and R.W. Murray, J. Electroanal. Chem., 94

(1978) 219; (b) R.J. Nowak, F.A. Schultz, M. Umaña, R. Lam and R.W. Murray, preprint; (c) P. Daum, J.R. Lenhard, D. Rolison and R.W. Murray, preprint.
12 F.B. Kaufman and E.M. Engler, J. Am. Chem. Soc., 101 (1979) 547.
13 (a) N. Oyama and F.C. Anson, J. Am. Chem. Soc., 101 (1979) 739; (b) Ibid., 3450.
14 F.B. Kaufman, A.H. Schroeder, E.M. Engler, S.R. Kramer and J.Q. Chambers, preprint.
15 J.B. Kerr and L.L. Miller, J. Electroanal. Chem., 101 (1979) 263.
16 A.F. Diaz, K.K. Kanazawa and G.P. Gardini, J. Chem. Soc. Chem. Commun., (1979) 635.
17 K. Huratsuka, H. Sasaki and S. Toshima, Chem. Lett., (1979) 751.
18 T.W. Smith, J.E. Kuder and D. Wychik, J. Polym. Sci.: Polym. Chem. Ed., 14 (1976) 2433.
19 (a) T. Gueshi, K. Tokuda and H. Matsuda, J. Electroanal. Chem., 89 (1978) 247; (b) Ibid., 101 (1979) 29; (c) K. Tokuda, T. Gueshi and H. Matsuda, ibid., 102 (1979) 41.
20 S. Gilman in A.J. Bard (Ed.), Electroanalytical Chemistry, Vol. 2, Marcel Dekker, New York, 1967, p. 1246.
21 K.H. Mancy, D.A. Okun, and C.N. Reilley, J. Electroanal. Chem., 4 (1962) 65.
22 S.K. Rangarajan and K.S.G. Doss, J. Electroanal. Chem., 5 (1963) 114.
23 R.C. Bowers and A.M. Wilson, J. Am. Chem. Soc., 80 (1958) 2968.
24 S.S. Fratoni, Jr. and S.P. Perone, Anal. Chem., 48 (1976) 287.
25 L.H. Lai Miaw and S.P. Perone, Anal. Chem., 51 (1979) 1645.
26 K.F. Dahnke, S.S. Fratoni, Jr. and S.P. Perone, Anal. Chem., 48 (1976) 296.
27 G.J. Janz and R.P.T. Tomkins, Nonaqueous Electrolytes Handbook, Vol. I, Academic Press, New York, 1972, p. 643.
28 F.M. Smits, Bell Syst. Tech. J., 37 (1958) 711.
29 H. Meier, Organic Semiconductors, Verlag Chemie, GmbH, D-694 Weinheim, 1974, p. 248.
30 R. Szentrimay, P. Yeh and T. Kuwana, paper presented at the 172nd National American Chemical Society Meeting, San Francisco, August 1976.
31 J.M. Bolts and M.S. Wrighton, J. Am. Chem. Soc., 101 (1979) 6179.
32 T. Tachikawa and L.R. Faulkner, J. Am. Chem. Soc., 100 (1978) 4379.
33 A. Erdelyi, W. Magnus, F. Oberhettinger, and F. Tricomi, Table of Integral Transforms, Vol. McGraw-Hill, New York, 1954, p. 246, formula no. 6.